X-RAYS GENERATION WITH A FEL BASED ON AN OPTICAL WIGGLER

A. Bacci, C. Maroli, L. Serafini, *INFN*-Sezione di Milano, 20133 Milano (Italy)
V. Petrillo , Dipartimento di Fisica dell'Università di Milano-INFN Sezione di Milano, 20133 Milano (Italy)
M.Ferrario , INFN-LNF, 00044 Frascati, Roma, Italy.

Abstract

The interaction between high-brilliance electron beams and counter-propagating laser pulses produces X rays via Thomson back-scattering. If the laser source is long and intense enough, the electrons of the beam can bunch and a regime of collective effects can be established. In the case of dominating collective effects, the FEL instability can develop and the system behaves like a free-electron laser based on an optical undulator. Coherent X-rays can be irradiated, with a bandwidth very much thinner than that of the corresponding incoherent emission. The main quantities that limit the brilliance of the X-rays are emittance, mean radius, current and energy spread of the electron beam, and the distribution and intensity of the laser beam. In this work we discuss first some ideal examples. Secondly we present the preparation of the electron beam by means of the use of a genetic code that optimizes the output of the code ASTRA. The electron beam obtained is analysed in slices and the best one is used in the 3-D radiation code.

INTRODUCTION

A Thomson back-scattering set-up can be considered in principle as a source of intense X-ray pulses which is at the same time easily tunable and highly monochromatic. Due to recent technological developments in the production of high brilliance electron beams and high power CPA laser pulses, it is now even conceivable to make steps toward their practical realisation.

The radiation generated in the Thomson back-scattering is usually considered incoherent and calculated by summing at the collector the intensities of the fields produced in single processes by each electron. If the laser pulse is long enough, however, collective effects can establish and become dominant. The system in this range of parameters behaves therefore like a free-electron laser, where the static wiggler is substituted by the optical laser pulse.

From the point of view of the theoretical description of the process, it is convenient to start with the same set of one-dimensional equations that are used in the theory of high-gain free-electron laser amplifier [1,2]. To take into account the many aspects of the process connected with the finite transverse geometry of the electron beam and of the laser and radiation pulses it is necessary to consider 3D equations [3].

A set of numerical results based on ideal electron beams is first presented. Secondly we present a genetic code that permits the optimization of the outputs of the beam dynamics code ASTRA, in order to obtain an electron beam with suitable characteristics. The electron beam obtained is analysed in slices and the best slice is used in the computation of the X-ray radiation under the effect of the laser. A short discussion of the importance of the data will be given at the end of the paper.

MODEL EQUATIONS AND IDEAL EXAMPLES

We start from the Maxwell-Lorentz equations that describe both laser and collective electromagnetic fields and from the relativistic equations of motion for the electrons of the beam. The laser and collective fields are given in terms of the corresponding scalar and vector potentials in the Coulomb gauge.

We assume that the laser is circularly polarised with the following form of the vector potential $\mathbf{A}_L$ (the laser pulse propagates along the z-axis in the negative direction):

$$\mathbf{A}_L(\mathbf{r},t) = \frac{a_{L0}}{\sqrt{2}}(g(\mathbf{r},t)e^{-i(k_L z+\omega_L t)}\hat{\mathbf{e}} + cc) + O(\frac{\lambda_L}{w_0}) \qquad (1)$$

where $\lambda_L = 2\pi/k_L$ is the laser wavelength, w_0 the laser spot size, $\omega_L=ck_L$ the angular frequency and $\hat{\mathbf{e}} = (\mathbf{e}_x + i\mathbf{e}_y)/\sqrt{2}$. The envelope g(**r**,t) is considered to be a slowly varying function of all variables xyz and t and is defined as a complex number with $|g(\mathbf{r},t)|\leq 1$. In the case of a laser pulse with a Gaussian transverse shape, the envelope has the form

$$g(r,t) = \Phi(z+ct)\frac{1+i\frac{z}{z_0}}{1+\frac{z^2}{z_0^2}} \exp\left[-4\frac{x^2+y^2}{w_0^2(1+\frac{z^2}{z_0^2})} - 4i\frac{x^2+y^2}{w_0^2(\frac{z}{z_0}+\frac{z_0}{z})}\right] \qquad (2)$$

where $z_0 = \pi w_0^2/4\lambda_L$ is the Rayleigh length and the form of the (real) function Φ (with $0\leq\Phi(z)\leq 1$) depends on the shape of the pulse along the z-axis. In the case of a guided laser pulse the quantity g(r,t) is a step function. We suppose that $\varphi(\mathbf{r},t)$ and $\mathbf{A}(\mathbf{r},t)$ have a slow dependence on x and y, i.e., that they vary on a transverse scale L_T much greater than the radiation wavelength $\lambda=2\pi/k$ and write, accordingly to the single-mode hypothesis frequently used in 1D treatments

$$\begin{aligned}\mathbf{A}(\mathbf{r},t) &= M(\mathbf{r},t)\hat{\mathbf{e}} + cc + O(\lambda/L_T) \\ &= A(\mathbf{r},t)e^{i(kz-\omega t)}\hat{\mathbf{e}} + cc + O(\lambda/L_T)\end{aligned} \qquad (3)$$

where $M(\mathbf{r},t) = A(\mathbf{r},t)e^{i(kz-\omega t)}$ and $\omega=ck$ is the radiation angular frequency. In the three-dimensional equation of

the model derived in details in Ref [3] a critical role is played by the FEL parameter $\rho = \frac{1}{\gamma_0}\left(\frac{\omega_b^2 a_{L0}^2}{16\omega_L^2}\right)^{\frac{1}{3}}$. The resonant frequency is at $\omega \approx \frac{4\gamma_0^2\omega_L}{1+a_{L0}^2}$. The fact that the quantum effects are negligible is guaranteed by taking the quantum parameter $q=\frac{\hbar k}{\rho mc<\gamma>} < 1$.

First, we have solved our model equations in the following case: the laser has a wavelength λ_L=10 micron and the parameter a_{L0} = 0.3. The diameter of the laser focal spot w_0 has been assumed 50 μm, the length of the pulse 70-100 psec, for a total power of 40-100 GW and a total energy of 4-10 J. The bunch of electrons has been chosen with an average value of γ, <γ>=60, corresponding to an energy of 30 MeV. This value of <γ> leads to a resonant wavelength λ=7.56 Angstrom. The quantum parameter q =0.2 and the classical model is expected to be fully valid. The collective effects appear and saturate after 7 gain lengths which in our case correspond to times of the order of 60-70 ps (each gain length corresponds to Lg=1 mm), i.e., of the same order of the duration of the laser pulse.

The electron beam has a mean radius σ_0=25 micron , a total charge of 1-5 nC and a length L_b= 1 mm, so that the Pierce parameter is $\rho=2.8\cdot10^{-4}$. Its energy spread $\Delta\gamma/\gamma$ ranges from 0 to $1.5\cdot10^{-4}$ and the initial normalized transverse emittance ε_n has been varied up to 1.

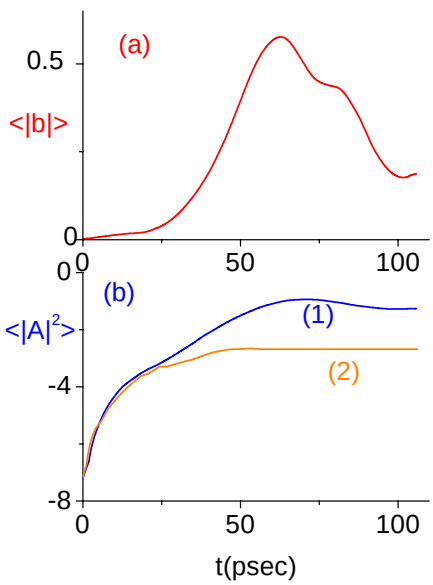

Figure 1 (a) |b| averaged on the transverse section *vs* t in psec and (b), (1) coherent value of $|A|^2(z_m)$ (b),(2) incoherent value for w_0= 50 μm, ε_n=0,6 mm mrad

Fig 1 shows the typical growth of the bunching factor in time (a), as well as the collective potential (b) curve 1 and the incoherent potential (b) curve 2. The amplitude of the vector potential $|A|^2$ has been calculated in the middle of the electron bunch at the position z_m =<z> and averaged on the transverse plane. The peak number of X coherent photons is $2.5\cdot10^{10}$, while the incoherent process provides $2\cdot10^{8}$ photons.

In this case w_0= 50 micron, ε_n=0,6 mm mrad, Q=3 nC, I=0.9 KA and the signal saturates at t=70 psec.

Figure 2 gives the first peak value of $<|A|^2>$ versus $\Delta\omega/(\omega\rho)$, representing the spectrum of the signal. As can be seen the width of the spectrum is few times ρ. In Fig 3 the peak value of $<|A|^2>$ is given as function of the transverse emittance, showing a depletion of the emission for emittances larger than 0.6-0.7 mm mrad.

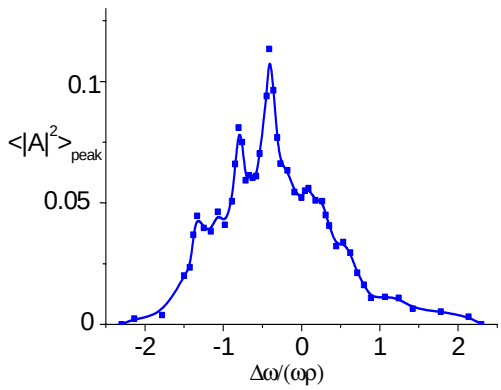

Figure 2: First peak value of $<|A|^2>$ versus $\Delta\omega/(\omega\rho)$ for the same parameters as Fig 1

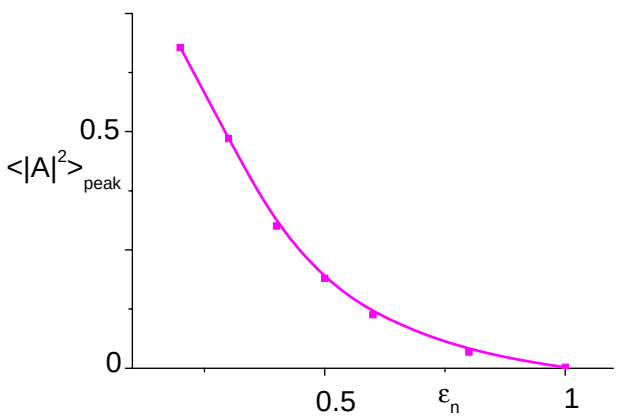

Figure 3: $<|A|^2>_{peak}$ versus ε_n evaluated in micron for the same case of Fig 1 and with $\Delta\omega/\omega=-10^{-4}$, w_0=50 micron, a_{L0}=0.3, $\Delta\gamma/\gamma=10^{-4}$.

In Figures 4,5,6,7 a different case is shown. The laser wavelength in this case is 0,8 μm.The electron beam has <γ>=30, for a Pierce parameter $\rho=4{,}38\cdot10^{-4}$. Other parameters of the beam are: a mean radius σ_0=10 micron, a total charge of 1 nC, a length L_b= 200 micron, corresponding to a beam current of I=1.5 KA.

In Fig 4 the bunching (a) and the collective (b) (1) and

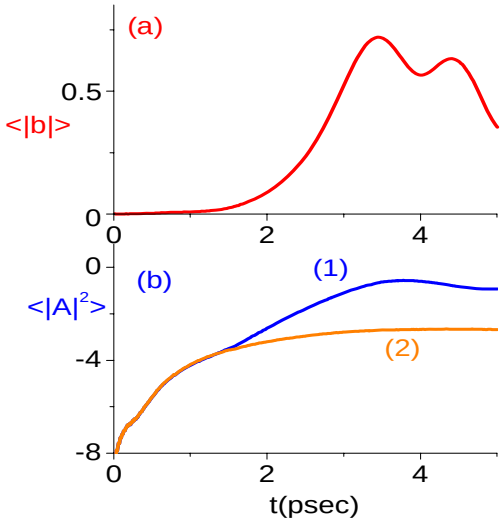

Figure 4: Bunching (a) and log of the radiation intensity (b) vs t in the coherent (1) and incoherent (2) case for: λ_L=0.8 μm, a_{L0}=0.8, $\Delta\gamma/\gamma=10^{-4}$,$\Delta\omega/\omega=-2\cdot10^{-4}$, ε_n=0.88.

incoherent (b) (2) potential amplitude are shown versus time. Furthermore, we have assumed a focal spot of radius w_0 of about 50 μm with a laser parameter of a_{L0}=0.8 so that the radiation turns out to have λ= 3,64 Angstrom. With these values the gain length corresponds to about 145 micron, the appearance and the saturation of the collective effects (taking place in 7-12 gain lengths) being contained in 5 picoseconds, a time of the same order of the duration of the laser pulse. The quantum parameter q is 0.5.

The energy spread $\Delta\gamma/\gamma$ of the electron beam has been chosen 1. 10^{-4} and the initial normalized transverse emittance has been varied from 0 up to 2.

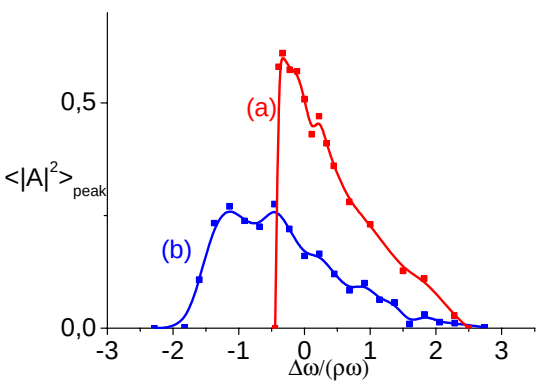

Figure 5: $\langle|A|^2\rangle_{peak}$ versus $\Delta\omega/(\omega\rho)$ for the case of fig 5 and (a) ε_n=0,44 μm and (b) ε_n=0,88 μm.

The saturation level of the radiation is reached at t=4 psec at $\langle|A|^2\rangle_{peak}$=0,275, with a total number of photons of 1,86 10^{10}, against the 2 10^8 provided by the incoherent process.

In Fig. 5 the spectrum of the radiation is presented, while in Fig. 6 the dependence of the maximum of $\langle|A|^2\rangle$ on the transverse normalized emittance is shown. Curve (a) is relevant to the situation of flat laser pulse with w_0=50 micron, while curve (b) shows the more critical situation where a Gaussian profile for the laser has been assumed. In this case the quantity σ_L has been taken equal to 106 μm with a_{L0}=0.8, increasing consequently the laser power.

We must note that we have considerable emission also in violation of the Pellegrini criterion for a static wiggler. In fact, the emittances considered exceed largely the value $\gamma\lambda/4\pi$, which in this case is $9\cdot10^{-4}$ μm. On the other hand, on the fact that $Z_R/Lg=1.2\cdot10^4$, the criterion of Pellegrini can be rewritten in a generalized form for both static and optical undulators as $\varepsilon_n \le \alpha\sqrt{Z_R/L_g}\lambda_R\gamma/4\pi$ [5] where $\alpha=\sqrt{d\omega/(\omega\rho)}\approx 2$, giving the more relaxed limit ε_n<0,3μ.

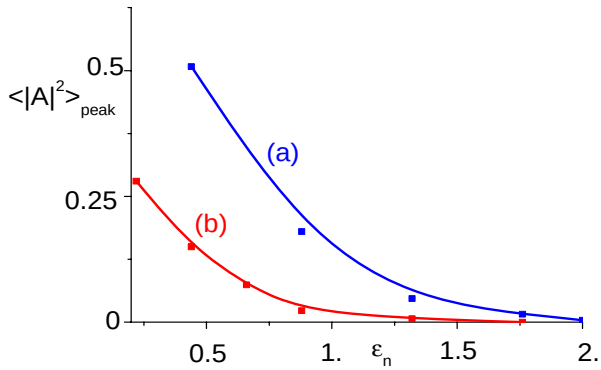

Figure 6: $\langle|A|^2\rangle_{peak}$ ves ε_n, with $\Delta\omega/\omega$=0. and: (a) flat laser profile with w_0=50 μm and a_{L0}=0.8 and (b) Gaussian laser profile with a_{L0}=0.8 and σ_L=106 μm.

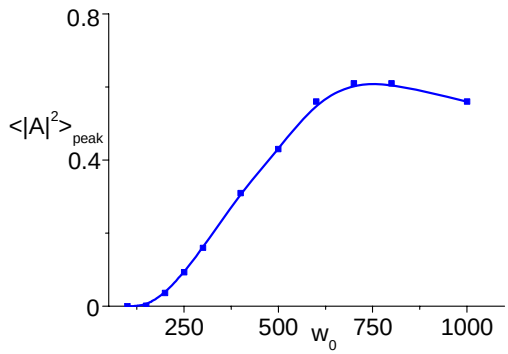

Figure 7 $\langle|A|^2\rangle_{peak}$ vs w_0 for a Gaussian laser for ε_n=0,44 μm, $\Delta\omega/\omega=-1\cdot10^{-4}$, a_{L0}=0.8.

Fig 7 shows the dependence of the growth of the signal on the transverse energy distribution of the laser in the case of a Gaussian pulse for ε_n=0,44 μm, $\Delta\omega/\omega=-1\cdot10^{-4}$, a_{L0}=0.8. In fact, in this case, a spot size with a radius smaller than 75 micron does not permit the instauration of the instability. The collective signal in this condition, therefore, does not grow.

REALISTIC EXAMPLE OBTAINED BY MEANS OF A GENETIC ALGORITHM

A realistic electron beam has been generated using the beam dynamic code ASTRA. The sequence of the accelerating and focalization elements in the beam line is shown in Fig 8, where the RF section works in the velocity bunching configuration.

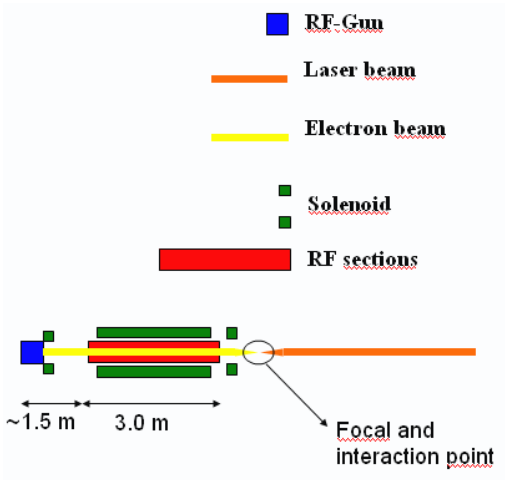

Figure 8: Beam line lay-out.

However, the optimization of the output is very difficult due to the high number of parameters which have to be fixed and to the non linear correlations existing between them. To circumvent this difficulty we have developed a genetic code that manages to fix the values of the parameters. The optimization is made by maximizing the following fitness function:

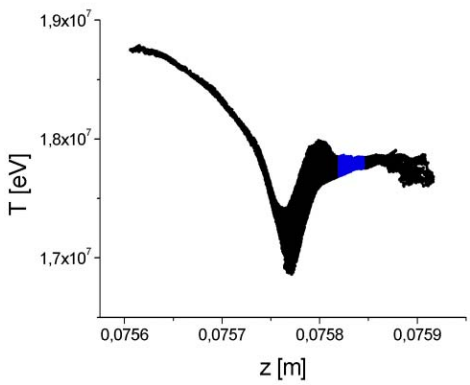

Figure 9: Bunch phase space and slice used (in blue).

$$F_{fitness} = \frac{I^{3.5}}{\varepsilon_{n-x,y} \cdot \sigma_{x,y} \cdot \sqrt{\left(\frac{\Delta\gamma}{\gamma}\right)}}$$

as function of the following genes defining the beam line: 1) Phase of the gun radiofrequency ϕ_{rf}. 2) Acceleration gradient in the bunching structure g_a. 3) Injection phase in the bunching structure ϕ_b. 4) Position of the bunching structure l_b. 5) Intensity of the first solenoid field B_1, used to control the envelope in the emittance compensation layout. 6) Intensity of the second solenoid field B_2, used to control the envelope. 7) Position of the second solenoid l_{s2}.

The convergence is reached in 500 generations on an electron beam configuration whose best slice has an emittance of 0,56 mm mrad, a radius of 15 micron, a length of 15 micron with a charge Q=0.05 nC. The genis values for the final configuration are: ϕ_{rf} =9.77°, g_a = 17.68 MV/m, ϕ_b =-91.57°, l_b =1.3868 m, B_1 =0.256 T B_2=0.0532 T, l_{s2} =1.3685m. The energy spread of the slice $\Delta\gamma/\gamma$ is 0.15 %. The growth of the signal is shown in fig 10, while the spectrum is in Fig 11. The saturation occurs in 6 psec, the focal spot size is w_0=30 μm, a_{L0}=0.8, for a total laser power of W=9.77 TW.

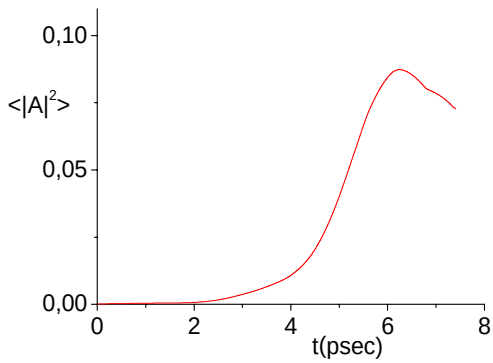

Figure 10: Growth of the signal.

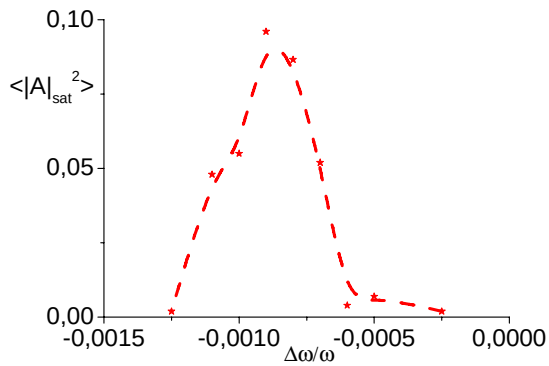

Figure 11: Spectrum of the signal.

REFERENCES

[1] W.B. Colson, Phys.Lett. 59A,187,(1976). R. Bonifacio, C. Pellegrini, L. Narducci Opt. Commun. 50 (1984) 313

[2] A.Bacci, C.Maroli, V.Petrillo, L.Serafini:"Collective effects in the Thomson back-scattering between a laser pulse and a relativistic electron beam" EPJAP (in print)

[3] A.Bacci, M.Ferrario, C. Maroli, V. Petrillo, L. Serafini PRST-AB 9 (2006) 060704